

A Compact Model of Polycrystalline Ferroelectric Capacitor

Chien-Ting Tung^{ID}, Graduate Student Member, IEEE, Girish Pahwa^{ID}, Member, IEEE, Sayeef Salahuddin^{ID}, Fellow, IEEE, and Chenming Hu^{ID}, Life Fellow, IEEE

Abstract—We present a compact model of polycrystalline ferroelectric (FE) capacitors. The polycrystalline thin-film material is modeled as a collection of independent grains or grain groups. Each grain or grain group is characterized by its local field-dependent switching rate, which is characterized by a distribution function such as Gaussian or type-2 generalized beta distribution. This computationally efficient model accurately reproduces the published experimental polarization switching waveforms and the switching current waveforms in response to all reported applied voltage waveforms. The model tracks the polarization history so that it can simulate the transition between major and minor and among minor loops as well as accumulative polarization which cannot be captured by the conventional models. This model is intended for simulating circuits containing FE capacitors using commercial SPICE simulators for arbitrary applied voltage waveforms. It also has the capability of simulating the discrete switching and device variability in small-area FE capacitors having a small number of grains, although there is no available experimental data to check the model accuracy in this regard.

Index Terms—Compact model, ferroelectric (FE), ferroelectric random access memory (FERAM), hafnium zirconium oxide (HZO).

I. INTRODUCTION

THE ferroelectricity in HfO_2 was discovered in 2011 [1], [2]. Due to its compatibility with the standard CMOS technology, ferroelectric (FE) HfO_2 thin films have been studied for their use in promising nonvolatile memories such as the FE random access memory (FERAM), FE field effect transistors, and FE tunnel junctions [3], [4]. The continuous nature and accumulation properties of FEs also make them suitable for neuromorphic applications [5]. In order to design and analyze these memory circuits, a compact model that can capture FE switching dynamics is therefore needed.

Manuscript received June 9, 2021; revised July 21, 2021; accepted July 26, 2021. Date of publication August 5, 2021; date of current version September 22, 2021. This work was supported by the Berkeley Device Modeling Center, University of California at Berkeley, Berkeley, CA, USA. The review of this brief was arranged by Editor A. M. P. Anantram. (Corresponding author: Chien-Ting Tung.)

The authors are with the Department of Electrical Engineering and Computer Sciences, University of California at Berkeley, Berkeley, CA 94720 USA (e-mail: cttung@berkeley.edu).

Color versions of one or more figures in this article are available at <https://doi.org/10.1109/TED.2021.3100814>.

Digital Object Identifier 10.1109/TED.2021.3100814

Several models have been proposed to describe the relation between the electric field and the switching time of the FE polarization. Kolmogorov–Avrami–Ishibashi (KAI) model is one of the widely used models among them [6], [7]. The KAI theory describes the polarization switching through unrestricted growth of reverse domains nucleated from different non-interacting nucleation centers in the FE material. Thus, KAI theory is ideally suitable only for the bulk FE materials and cannot describe polycrystalline FEs with multiple grains such as those based on doped HfO_2 [8]. Therefore, another theory called inhomogeneous field mechanism (IFM) or nucleation-limited switching (NLS) model was proposed to model the polycrystalline FEs [9]–[14]. These models assume that there are many small grains in the FE material and each grain has its own switching time which is determined by the local material properties. This local switching time is assumed to follow some statistical distribution.

The polarization expressions as function of time and electric field used in these models are arrived at by assuming a constant electric field. These models have been shown to fit the experimental data of hafnium zirconium oxide (HZO) under a constant voltage pulse, but they are not able to handle arbitrary input signals. Furthermore, these models assume the polarization reversal starts from the fully polarized state. Thus, they cannot model the minor loop switching and accumulation properties [15]. Other models such as Preisach model need to use empirical interpolation and scaling of model parameters to produce the partial switching, which is not physical [16]–[18]. Although with more intensive phase-field-based Landau models, the accuracy of the simulations can be improved, they are computationally expensive and therefore not very useful for simulation of real circuits containing a large number of FE memory elements [19].

In order to simulate FE under arbitrary inputs, a model using Monte Carlo simulation was proposed in [20]. Based on multi-grain dynamics, the FE is divided into many small physical grains and each grain has its own switching probability. By introducing an accumulated time constant, the model could handle arbitrary waveforms and showed the accumulative polarization reversal [17], [18]. However, this modeling framework is computationally intensive. The usual number of the physical grains in the FE material is up to hundreds or thousands. To achieve the much higher computational efficiency required for simulating integrated circuits, this brief

presents a compact model of polycrystalline FE capacitors that can capture the switching dynamics of FE under arbitrary input waveforms in good agreement with experimental results and computationally suitable for circuit design purposes.

II. MODEL

We assume that the FE film consists of many crystalline grains or grain groups. Each group is characterized by a material parameter η , which characterizes the random variation of the local switching rates in (2) such as the variations in crystal grain orientation, stress, or stoichiometry. The area of the grain or grain group that has a material parameter η is A_η whose value is total film area A_T times the probability of η , $P(\eta)$. Part of A_η is positively polarized and the rest is negatively polarized. The positively polarized area is denoted as $A_{\eta+}$ and the negatively polarized area is $A_{\eta-}$. The positively and negatively polarized areas can increase or decrease with time under an applied voltage. However, their sum is always A_η . Assume that a positive voltage is applied. Previously published models and experimental studies show that the growth of $A_{\eta+}$ follows an exponential time dependence at a fixed positive applied voltage. This suggests that the rate equation of polarization switching of the FE material is a simple first-order differential equation as

$$\begin{aligned} \frac{dA_{\eta+}}{dt} &= \frac{A_\eta - A_{\eta+}}{\tau(t, \eta)}, \quad \text{if } E_{FE}(t) \geq 0 \\ &= \frac{-A_{\eta+}}{\tau(t, \eta)}, \quad \text{if } E_{FE}(t) < 0. \end{aligned} \quad (1)$$

The value of η is experimentally observed between 0 and 2 with a statistical distribution and a unity mean [11], [18]. Therefore, our model limits η from 0 to 2. It influences the switching characteristic time $\tau(t, \eta)$ given by the Merz's law [11], [13], [14] as

$$\tau(t, \eta) = \tau_0 \exp\left(\left(\frac{\eta E_a}{|E_{FE}(t)|}\right)^\alpha\right) \quad (2)$$

where E_a is the activation field which can be used as a fitting parameter to fit experimental data or be substituted with a theoretical value, E_{FE} is the applied electric field, τ_0 is the characteristic time for a very large E_{FE} , and α is a fitting parameter.

By solving (1), we obtain (3) where the integration of $1/\tau(t, \eta)$ tracks the applied electric field

$$\begin{aligned} A_{\eta+}(t) &= A_\eta - (A_\eta - A_{\eta+})|_{t=t_i} \exp\left(-\left(\int_{t_i}^t \frac{1}{\tau(t', \eta)} dt'\right)^\beta\right), \\ &\quad \text{if } E_{FE}(t) \geq 0 \\ &= A_{\eta+}|_{t=t_i} \exp\left(-\left(\int_{t_i}^t \frac{1}{\tau(t', \eta)} dt'\right)^\beta\right), \quad \text{if } E_{FE}(t) < 0. \end{aligned} \quad (3)$$

Equation (3) is different from the NLS theory which assumes a constant electric field [10], [12]. An empirical parameter β is introduced to (3) to improve fitting with experimental data [18]. At the beginning of the simulation $t = 0$, the initial condition for $A_{\eta+}$ is specified by the user.

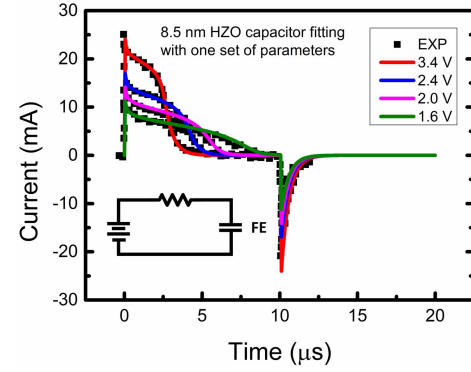


Fig. 1. Modeled current waveforms versus time for several voltages of a 8.5-nm HZO capacitor agree with experimental data from [13] with $P_R = 20 \mu\text{C}/\text{cm}^2$, $\tau_0 = 100 \text{ ps}$, $E_a = 8.0 \text{ MV}/\text{cm}$, and a 135Ω series resistance. These parameters are the same as used in [13].

t_1 is the time instant when E_{FE} polarity changes for the first time. The second time when E_{FE} polarity changes is called t_2 . Similarly, t_i is the i th time when E_{FE} polarity changes.

Now, we sum up all the $A_{\eta+}$. We assume η is continuous. Thus, $P(\eta)$ becomes $f(\eta)d\eta$ where $f(\eta)$ is the probability distribution function (PDF), and summation becomes an integration as

$$A_+(t) = \sum A_{\eta+}(t) \cong \int_0^{\eta_{\max}} A_T f(\eta) d\eta \times \frac{A_{\eta+}(t)}{A_\eta}. \quad (4)$$

Previous experimental studies have identified two common PDFs, the Gaussian PDF [13], [14], and the generalized beta distribution of type 2 (GB2) [11], [18]. We carry out a numerical integration with 80 points to compute (4) which is more efficient when compared to [18] that uses thousands of grains to achieve the accuracy as shown in the following section. Finally, the polarization is calculated as

$$P(t) = P_R \times \left(\frac{2A_+(t)}{A_T} - 1\right) \quad (5)$$

where P_R is the remanent polarization and the switching current is obtained by the time differential of (5). The total current is the combination of the switching current and the current from the background dielectric as

$$I(t) = 2P_R \frac{dA_+(t)}{dt} + C_{FE} \frac{dV_{FE}}{dt}. \quad (6)$$

III. MODEL VALIDATION

We implement our model with Verilog-A code and validate it with different experimental data. In Fig. 1, we fit the experimental switching current data from [13] which is a 8.5-nm HZO capacitor. The model parameters are extracted for the given FE thickness and should be re-extracted when the thickness is changed. Here, we apply a Gaussian distribution with a mean at 1 and standard deviation, $\sigma = 0.32$ for $f(\eta)$. As shown, our model can accurately capture the experimental data for different amplitudes of the applied voltage.

We also validate our model with the experimental data from [18]. First, the P - t data of an 8.3-nm HZO capacitor for different amplitudes of applied voltage pulses is fitted in Fig. 2

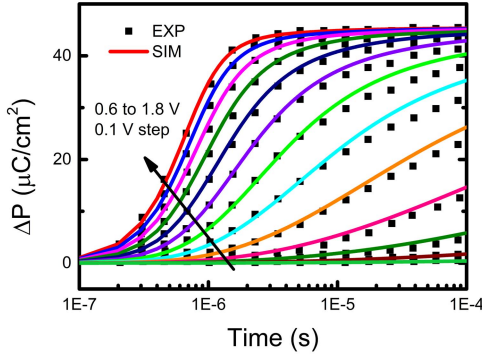


Fig. 2. Fitted P - t curves of a 8.3-nm HZO capacitor from [18] with $P_R = 22.9 \mu\text{C}/\text{cm}^2$, $\tau_0 = 390 \text{ ps}$, $E_a = 1.74 \text{ MV}/\text{cm}$, $\alpha = 3.48$, $\beta = 2.0$, and a offset voltage of -0.08 V .

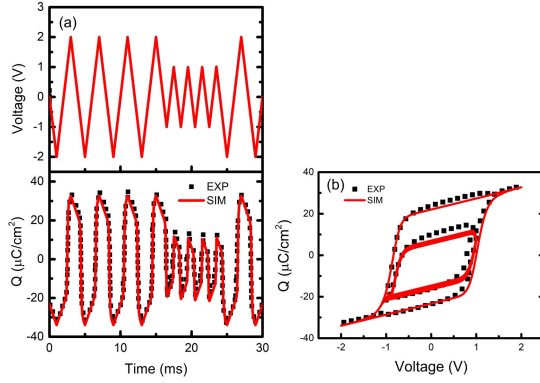


Fig. 3. (a) Simulation for the FE capacitor while applying a triangular waveform using the parameters extracted from Fig. 2. (b) Comparison between the experimental and simulated P - V curve from the voltage pulse shown in Fig. 3(a). The difference between the two data comes from assumption of the constant permittivity.

by using a GB2 PDF given by (7) with $a = 2.1$, $b = 0.99$, $p = 0.691$, and $q = 0.633$

$$\text{GB2}(\eta) = \frac{|a|b(b\eta)^{ap-1}}{B(p, q)[1 + (b\eta)^a]^{p+q}} \quad (7)$$

where $B(p, q)$ denotes the beta function. It shows that the model can capture the transient properties of the FE capacitor under different electric fields. Then, the same parameter set is used to test the model capability to handle arbitrary input signals. GB2 PDF is a more general distribution and can fit the η distribution that the Gaussian PDF cannot handle. One should choose the suitable PDF depending on the extracted distribution from experimental data [10], [11].

We apply the same triangular voltage waveform with varying amplitude as in [18] and shown in Fig. 3(a). The simulated charge closely matches the experimental data. By transforming Q - t into Q - V curves in Fig. 3(b), we can see that our model can capture the transition between the major loop and minor loop switching and very well tracks the history of the FE device. The differences between the experiment and simulation could be because of a constant background permittivity assumption used in this model. Furthermore, we test the accumulative polarization property. Accumulation happens when a pulse train is applied to the FE. The polarization would gradually increase with the number of pulses. In Fig. 4, pulse trains with $1 \mu\text{s}$ pulsewidth are applied to the FE

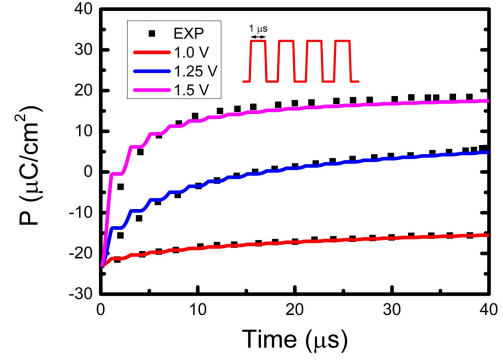


Fig. 4. Validation of the polarization accumulation by comparing the simulation results with the measurement in [18]. Pulse trains with $1 \mu\text{s}$ pulsewidth at different amplitudes are applied to the capacitor.

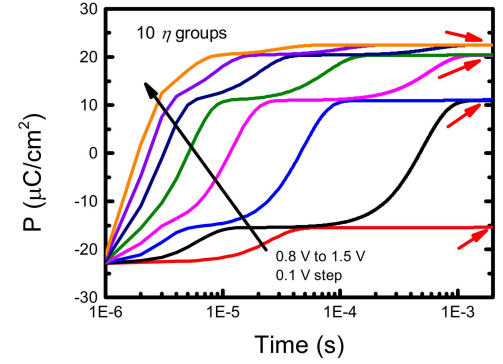


Fig. 5. Discrete switching behavior for a device with 10 η groups. There are four states for this device different from the continuous states in large-area capacitor as Fig. 2.

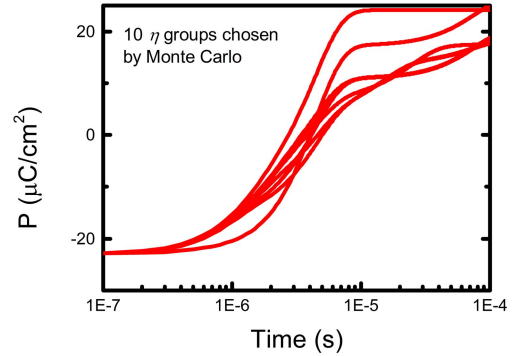


Fig. 6. Simulation of 10 devices with 10 η groups which has a large device variability.

capacitor. It shows that our simulation results can also fit the experimental data of polarization accumulation well.

IV. SCALABILITY

We have verified our model with the large-area capacitor data. In a small-area device, the limited number of the grains would make the η groups become discrete and cause discrete switching [21]. Normally, we use 80 η groups in integration to approximate the continuous distribution of η . By reducing the number of η groups, we can model the discrete switching and device variation seen in scaled FE capacitors [17], [18], [22]. Fig. 5 shows discrete states of polarization in a small-area FE capacitor which contains only 10 η groups. The switching has abrupt jumps and there are only four final states which are different from the continuous switching shown in Fig. 2. It is

because the local activation fields are discrete. Small applied voltage pulses can only switch a part of the FE irrespective of how long the time is. If the voltage is increased to above a certain value, it can switch another part of the FE causing the abrupt switching state, and so on. In this case, some η groups might have very small η , so basically every voltage can switch them. There are just four η groups that can induce discrete switching. We also test the variability in a small-area FE capacitor in Fig. 6. It shows that there is a large variation among several devices.

It is because, on a large-area capacitor, η approximately follows a continuous probability distribution. If we cut this capacitor into many small-area capacitors, these capacitors would only contain some part of the η , and each capacitor would have different η groups on it. It leads to device variability. Although this model exhibits these properties seen in small-area devices, its assumption of the independent switching of each grain does not hold for small-area FE. More data are needed to verify and improve the model for the application to small devices.

V. CONCLUSION

We have developed a compact model of FE capacitors based on the experimental observation of polarization switching in polycrystalline materials. This model can capture the switching dynamics under arbitrary input waveforms like minor loop switching as well as polarization accumulation and is therefore suitable for modeling FE memory devices together with the write and read circuits using any circuit simulators. Although, for small-area FE capacitors, the assumptions of this model are not entirely correct, the model can still simulate discrete switching and device variations, which points out its potential for high-density FERAM simulations.

REFERENCES

- [1] T. S. Böske, J. Müller, D. Bräuhäus, U. Schröder, and U. Böttger, "Ferroelectricity in hafnium oxide thin films," *Appl. Phys. Lett.*, vol. 99, no. 10, Sep. 2011, Art. no. 102903, doi: [10.1063/1.3634052](#).
- [2] T. S. Böske; J. Müller; D. Bräuhäus; U. Schröder; U. Böttger, "Ferroelectricity in hafnium oxide CMOS compatible ferroelectric field effect transistors," in *IEDM Tech. Dig.*, Washington, DC, USA, Dec. 2011, pp. 1–24.
- [3] A. I. Khan, A. Keshavarzi, and S. Datta, "The future of ferroelectric field-effect transistor technology," *Nature Electron.*, vol. 3, no. 10, pp. 588–597, Oct. 2020, doi: [10.1038/s41928-020-00492-7](#).
- [4] A. Keshavarzi, K. Ni, W. Van Den Hoek, S. Datta, and A. Raychowdhury, "Ferroelectronics for edge intelligence," *IEEE Micro*, vol. 40, no. 6, pp. 33–48, Nov. 2020, doi: [10.1109/MM.2020.3026667](#).
- [5] E. W. Kinder, C. Alessandri, P. Pandey, G. Karbasian, S. Salahuddin, and A. Seabaugh, "Partial switching of ferroelectrics for synaptic weight storage," in *Proc. 75th Annu. Device Res. Conf. (DRC)*, South Bend, IN, USA, Jun. 2017, pp. 1–12.
- [6] Y. Ishibashi and Y. Takagi, "Note on ferroelectric domain switching," *J. Phys. Soc. Jpn.*, vol. 31, no. 2, pp. 506–510, 1971, doi: [10.1143/JPSJ.31.506](#).
- [7] M. Avrami, "Kinetics of phase change. I General theory," *J. Chem. Phys.*, vol. 7, no. 12, pp. 1103–1112, Dec. 1939, doi: [10.1063/1.1750380](#).
- [8] I. Stolichnov, L. Malin, E. Colla, A. K. Tagantsev, and N. Setter, "Microscopic aspects of the region-by-region polarization reversal kinetics of polycrystalline ferroelectric Pb(Zr,Ti)O₃ films," *Appl. Phys. Lett.*, vol. 86, no. 1, Jan. 2005, Art. no. 012902, doi: [10.1063/1.1845573](#).
- [9] A. K. Tagantsev, I. Stolichnov, N. Setter, J. S. Cross, and M. Tsukada, "Non-Kolmogorov-Avrami switching kinetics in ferroelectric thin films," *Phys. Rev. B, Condens. Matter*, vol. 66, no. 21, Dec. 2002, Art. no. 214109, doi: [10.1103/PhysRevB.66.214109](#).
- [10] X. J. Lou, "Statistical switching kinetics of ferroelectrics," *J. Phys., Condens. Matter*, vol. 21, no. 1, 2009, Art. no. 012207, doi: [10.1088/0953-8984/21/1/012207](#).
- [11] C. Alessandri, P. Pandey, A. Abusleme, and A. Seabaugh, "Switching dynamics of ferroelectric Zr-doped HfO₂," *IEEE Electron Device Lett.*, vol. 39, no. 11, pp. 1780–1783, Nov. 2018, doi: [10.1109/LED.2018.2872124](#).
- [12] N. Gong, X. Sun, H. Jiang, K. S. Chang-Liao, Q. Xia, and T. P. Ma, "Nucleation limited switching (NLS) model for HfO₂-based metal-ferroelectric-metal (MFM) capacitors: Switching kinetics and retention characteristics," *Appl. Phys. Lett.*, vol. 112, no. 26, Jun. 2018, Art. no. 262903, doi: [10.1063/1.5010207](#).
- [13] S. D. Hyun *et al.*, "Dispersion in ferroelectric switching performance of polycrystalline Hf_{0.5}Zr_{0.5}O₂ thin films," *ACS Appl. Mater. Interface*, vol. 10, no. 41, pp. 35374–35384, Oct. 2018, doi: [10.1021/ACSAMI.8b13173](#).
- [14] S. Zhukov, Y. A. Genenko, and H. von Seggern, "Experimental and theoretical investigation on polarization reversal in unfatigued lead-zirconate-titanate ceramic," *J. Appl. Phys.*, vol. 108, no. 1, Jul. 2010, Art. no. 014106, doi: [10.1063/1.3380844](#).
- [15] H. Mulaosmanovic, T. Mikolajick, and S. Slesazek, "Accumulative polarization reversal in nanoscale ferroelectric transistors," *ACS Appl. Mater. Interfaces*, vol. 10, no. 28, pp. 23997–24002, Jun. 2018, doi: [10.1021/ACSAMI.8b08967](#).
- [16] K. Ni, M. Jerry, J. A. Smith, and S. Datta, "A circuit compatible accurate compact model for ferroelectric-FETs," in *Proc. IEEE Symp. VLSI Technol.*, Honolulu, HI, USA, Jun. 2018, pp. 131–132.
- [17] S. Deng *et al.*, "A comprehensive model for ferroelectric FET capturing the key behaviors: Scalability, variation, stochasticity, and accumulation," in *Proc. IEEE Symp. VLSI Technol.*, Honolulu, HI, USA, Jun. 2020, pp. 1–2.
- [18] C. Alessandri, P. Pandey, A. Abusleme, and A. Seabaugh, "Monte Carlo simulation of switching dynamics in polycrystalline ferroelectric capacitors," *IEEE Trans. Electron Devices*, vol. 66, no. 8, pp. 3527–3534, Aug. 2019, doi: [10.1109/TED.2019.2922268](#).
- [19] A. K. Saha, K. Ni, S. Dutta, S. Datta, and S. Gupta, "Phase field modeling of domain dynamics and polarization accumulation in ferroelectric HZO," *Appl. Phys. Lett.*, vol. 114, no. 20, May 2019, Art. no. 202903, doi: [10.1063/1.5092707](#).
- [20] C. Alessandri, P. Pandey, and A. C. Seabaugh, "Experimentally validated, predictive Monte Carlo modeling of ferroelectric dynamics and variability," in *IEDM Tech. Dig.*, San Francisco, CA, USA, Dec. 2018, pp. 1–16.
- [21] H. Mulaosmanovic, J. Ocker, S. Müller, U. Schroeder, J. Müller, P. Polakowski, S. Flachowsky, R. van Bentum, T. Mikolajick, and S. Slesazek, "Switching kinetics in nanoscale hafnium oxide based ferroelectric field-effect transistors," *ACS Appl. Mater. Interfaces*, vol. 9, no. 4, pp. 3792–3798, Feb. 2017, doi: [10.1021/ACSAMI.6b13866](#).
- [22] R. Xu *et al.*, "Kinetic control of tunable multi-state switching in ferroelectric thin films," *Nature Commun.*, vol. 10, no. 1, p. 1282, Mar. 2019, doi: [10.1038/s41467-019-09207-9](#).